Cell-specialized chloroplast signaling orchestrates photosynthetic and extracellular reactive oxygen species for stress responses

Estee E. Tee[1,5], Stephen J. Fairweather[1], Hanh M. Vo[1,6], Chenchen Zhao[2,7], Andrew Breakspear[3], Sachie Kimura[4,8], Melanie Carmody[4,9], Michael Wrzaczek[4,10], Stefan Broer[1], Christine Faulkner[3], Jaakko Kangasjärvi[4], Zhong-Hua Chen[2], Barry J. Pogson[1*], Kai Xun Chan[1*]

[1]Research School of Biology, Australian National University, 2601 Canberra, Australia

[2]School of Science, Western Sydney University, 2753 Sydney, Australia

[3]Cell and Developmental Biology, John Innes Centre, NR4 7UH Norwich, United Kingdom

[4]Organismal and Evolutionary Biology, Viiki Plant Science Centre, University of Helsinki, 00014 Helsinki, Finland

[5]Present address: Cell and Developmental Biology, John Innes Centre, NR4 7UH Norwich, United Kingdom

[6]Present address: School of Natural Sciences, University of Tasmania, 7001 Hobart, Australia

[7]Present address: Tasmanian Institute of Agriculture, University of Tasmania, 7250 Launceston, Australia

[8]Present address: NAPIGEN, Inc., 19803 Delaware, United States of America

[9]Present address: Synthetic Biology Future Science Platform, Commonwealth Scientific and Industrial Research Organisation, 2601 Canberra, Australia

[10]Present address: Institute of Plant Molecular Biology, Czech Academy of Sciences, 370 05 České Budějovice, Czech Republic

[*] **Authors for Correspondence:** kai.chan@anu.edu.au and barry.pogson@anu.edu.au

Author Contributions: E.E.T., S.J.F., S.K., M.C., M.W., S.B., C.F., J.K., Z.H.C., B.J.P. and K.X.C. designed research; E.E.T., S.J.F., H.M.V., C.Z., and A.B. performed research; E.E.T., S.J.F., H.M.V. analyzed data; E.E.T., B.J.P., and K.X.C. wrote the paper with contribution from all authors.

Competing Interest Statement: No competing interests to declare.

Classification: Biological Sciences; Plant Biology

Keywords: Chloroplast, ROS, retrograde signaling, stomata, calcium dependent protein kinase

This PDF file includes:

Main Text

Figures 1 to 4

Abstract

Cellular responses to abiotic stress involve multiple secondary messengers including reactive oxygen species (ROS), Ca^{2+}, phytohormones such as abscisic acid (ABA) and chloroplast-to-nucleus retrograde signals such as 3'-phosphoadenosine 5'-phosphate (PAP). Mechanism(s) by which these messengers, produced in different subcellular compartments, intersect for cell regulation remain enigmatic. Here we demonstrate a mechanistic link enabling ABA and the chloroplast retrograde signal PAP to coordinate both chloroplast and plasma membrane ROS production. In whole leaves, PAP alters various ROS-related processes including plasmodesmal permeability as well as responses to ozone and the bacterial elicitor flg22, but largely quenches ROS during oxidative stress. Conversely, in guard cells, both PAP and ABA induce a ROS burst in both chloroplasts via photosynthetic electron transport, and the apoplast via the RESPIRATORY BURST OXIDASE HOMOLOG (RBOH). Both subcellular ROS sources were necessary for ABA- and PAP-mediated stomatal closure. However, PAP signaling diverges from ABA by activating RBOHD, instead of RBOHF, for apoplastic ROS production. We identify calcium-dependent protein kinases (CPKs) transcriptionally induced by PAP as the post-translational activators of RBOHD-mediated ROS production. CPK13, CPK32, and CPK34 concurrently activate RBOHD and the slow anion channel SLAC1 by phosphorylating two Serine (S) residues, including S120 which is also targeted by the core ABA signaling kinase OPEN STOMATA 1 (OST1). Consequently, overexpressing the PAP-induced CPKs rescues stomatal closure in *ost1.* Our data identify chloroplasts, as sources and mediators of ROS and retrograde signals such PAP, to be critical environmental sensors and focal node in the multifaceted cellular stress response network.

Significance Statement

The chloroplast is an important node to coordinate multiple plant signaling pathways in response to stresses such as drought. However, how does it function in specialized cells for which carbon fixation is secondary? Here we show that the chloroplast retrograde signal 3'-phosphoadenosine 5'-phosphate (PAP) plays multiple roles in reactive oxygen species (ROS) signaling and

homeostasis. While PAP suppresses ROS in photosynthetic tissue, surprisingly PAP induces ROS in chloroplasts and extracellular space of guard cells to induce stomatal closure. We decipher how PAP-induced proteins activate both extracellular ROS production and anion channels for stomatal closure, thus providing a mechanism by which chloroplasts provide a strategic complement to canonical hormonal pathways in regulating plant physiological responses in specialized cells.

67 **Main Text**

68

69 **Introduction**

70

71 Plant cell responses to abiotic and biotic stresses involve a suite of coordinated cellular signaling
72 cascades. These involve multiple messenger molecules including reactive oxygen species (ROS),
73 calcium ions (Ca^{2+}), phytohormones such as abscisic acid (ABA), and organelle-to-nucleus
74 retrograde signals, defined as signals from an organelle (i.e., the chloroplast or mitochondria) that
75 regulate nuclear gene expression (1–3). While each of the aforementioned messengers have been
76 extensively studied, their spatio-temporal intersections remain enigmatic. For example, both
77 apoplastic ROS and organelle-to-nucleus retrograde signals occur concurrently, yet it is unclear
78 how these two classes of signals interact and are coordinated in specialized cells.

79

80 ROS are crucial signaling molecules produced in diverse subcellular compartments including
81 chloroplasts and the apoplast. Several types of ROS exist in plant cells and distinct ROS types play
82 different signaling roles (1–3), but herein we refer to chloroplast and apoplast "ROS" as an
83 encompassing term for three ROS types formed via similar mechanisms at these subcellular
84 locations: superoxide (O_2^-), its dismutation product hydrogen peroxide (H_2O_2), and hydroxyl radical
85 ($OH\cdot$); with H_2O_2 being the most stable (1). ROS generated from photosystem I (PSI) in chloroplasts
86 participates in chloroplast-to-nucleus retrograde signaling, both by triggering production of
87 retrograde signals via H_2O_2-responsive redox regulation (4) and by itself acting as a retrograde
88 signal (5). Silencing the chloroplastic H_2O_2 scavenging enzyme, thylakoid membrane-bound
89 ascorbate peroxidase (tAPX), increased chloroplastic H_2O_2 leading to the up-regulation of multiple
90 stress-associated genes, including pathogen-responsive genes in photosynthetic tissues (6). High
91 light stress increases H_2O_2 production in leaf chloroplasts; the chloroplasts in close physical
92 association with the nucleus can transfer their H_2O_2 into the nucleus, potentially representing a

93 direct means for H_2O_2 to act as a retrograde signal to induce nuclear gene expression (5). However,
94 the nuclear target(s) of the chloroplast sourced H_2O_2 are still unknown.
95
96 In contrast to chloroplast PSI ROS, apoplastic superoxide and H_2O_2 are known to act as secondary
97 messengers in dynamic signaling cascades. A well characterized pathway that utilizes apoplastic
98 and cellular ROS as a secondary messenger is abscisic acid (ABA)-mediated stomatal closure. In
99 a response to an accumulation of ABA under stress conditions such as drought, a simplified guard
100 cell process occurs as follows: ABA forms a complex with PYRABACTIN RESISTANCE 1/PYR1-
101 LIKE/REGULATORY COMPONENTS OF ABA RECEPTORS, with ABSCISIC ACID-
102 INSENSITIVE 1 (ABI1) PP2C phosphatase then binding to the complex (7, 8). This removes the
103 inhibition of SUCROSE NON-FERMENTING-1 RELATED PROTEIN KINASE (SnRK) 2.6 (SnRK
104 2.6)/SRK2E/OPEN STOMATA 1 (OST1), which can auto-phosphorylate (9, 10). OST1 interacts
105 with RESPIRATORY BURST OXIDASE HOMOLOG F (RBOHF) (11) and RBOHD (12), leading to
106 RBOH-mediated ROS (superoxide and H_2O_2) production. OST1 also directly regulates the activity
107 of multiple ion channels by phosphorylation, including activation of SLOW ANION CHANNEL 1
108 (SLAC1) and rapid type anion channel ALMT12 (12–14), and inhibiting inward rectifying
109 POTASSIUM CHANNEL (KAT1) (15). While OST1 has the capacity to directly act on the channels,
110 both ROS and cytosolic Ca^{2+} are required for stomatal closure with H_2O_2 activating Ca^{2+} channels
111 to induce the influx of Ca^{2+} and release of Ca^{2+} from vacuoles and other organelles to the cytosol
112 (16–18).
113
114 ROS production via RBOHs is regulated by a suite of different kinases at the whole leaf, tissue,
115 cellular and organellar levels. The Ca^{2+} sensor CALCINEURIN B-LIKE proteins (CBL1; CBL9)
116 interact with CBL-INTERACTING PROTEIN KINASE (CIPK11; CIPK26) to activate RBOHF (19).
117 In contrast, RBOHD is the primary apoplastic ROS generator in response to biotic stimuli and
118 mechanical wounding (20, 21). Regulators of RBOHD activity include several immunity-associated
119 protein kinases (22–24), and calcium protein kinases (CPKs). CPK1, CPK2, CPK4, CPK5, CPK6

120 and CPK11 can activate both RBOHD and RBOHF in an immunocomplex kinase assay (25), and
121 at least for CPK5, a direct interaction and activation of RBOHD has been confirmed (26). In guard
122 cells, OST1 activating RBOHF is thought to be the primary pathway for apoplastic ROS production
123 (11, 18). However, the links between ROS production and CPKs as well as the interaction with
124 retrograde signals and the production of apoplastic ROS in guard cells remain elusive, if not illogical
125 from a spatial context.
126
127 The aforementioned leaf chloroplast PSI ROS can trigger other chloroplast-to-nucleus retrograde
128 signaling pathways such as the SAL1-PAP (3'phosphoadenosine 5'phosphate) retrograde
129 signaling pathway that functions in drought and high light stress. These abiotic stresses promote
130 chloroplast PSI ROS and redox poise which inhibit plastidial SAL1 activity (4), thus allowing
131 accumulation of its catabolic substrate PAP in the cell. In the nucleus, PAP inhibits 5' to 3'
132 exoribonucleases to alter RNA polymerase II function. This leads to read through accumulation of
133 downstream genes in tandem repeats, resulting in accumulation of stress-responsive transcripts
134 including H_2O_2 scavengers (27, 28). Consequently, *sal1* mutants with constitutively over-
135 accumulated PAP show lower foliar ROS levels, particularly in the vascular bundle (29).
136
137 In guard cells, the SAL1-PAP pathway functions in parallel to the canonical ABA signaling
138 (RCAR/PYL-OST1-PP2C) pathway to induce stomatal closure, at least in part via transcriptional
139 upregulation of CPKs which converge upon, and activate, OST1 target proteins such as the SLAC1
140 anion channel (30). Intriguingly, PAP appears to have contrasting effects on ROS in different cell
141 types. While constitutive PAP accumulation leads to decreased ROS in vascular bundles,
142 exogenous PAP application induces a ROS burst in guard cells, perhaps via RBOHs as indicated
143 by chemical inhibitor experiments (30). Constitutively accumulated PAP also rescues ABA-induced
144 ROS burst in *ost1 sal1* guard cells (30). However, the mechanism was not investigated, beyond
145 establishing that most canonical ABA signaling components were activated by PAP in *ost1* mutants.
146

147 These contrasting roles for PAP as an initiator and repressor of ROS signaling raise the hypothesis
148 tested herein that chloroplasts and their retrograde signals can function differently depending on
149 cellular context. Further, despite the parallels in chloroplast-sourced retrograde ROS signaling and
150 apoplast-sourced secondary messenger ROS signaling, there is a distinct lack of knowledge how
151 these two processes are intertwined in stress signaling. In this work we explore how SAL1-PAP
152 retrograde signaling intersects with whole-leaf ROS responses such as basal plasmodesmal
153 permeability, flg22-induced ROS responses and tolerance to ozone-derived apoplastic ROS. To
154 define how PAP, and consequently chloroplastic signals, can intersect with ROS signaling, we use
155 the guard cell as a model to study the specializations of each pathway. This includes considerations
156 of the sites of ROS bursts, phosphorylation targets of CPKs and the extent to which ABA-mediated
157 and PAP-mediated signaling require chloroplast functionality as well as retrograde signaling for
158 stomatal closure.
159
160 **Results**
161 *Subcellular guard cell ROS compartmentalization is mediated by retrograde signaling for stomatal*
162 *closure*
163 Previously, we showed that ROS signaling was restored by PAP in ABA signaling mutants, but we
164 did not determine the cellular source of ROS nor its regulation (30). Herein we examined the spatial
165 distribution of ROS in response to exogenous PAP application and observed that PAP elevated
166 ROS in multiple subcellular compartments, with a notable and significant increase in chloroplasts
167 as indicated by fluorescence of H_2DCFDA, which detects primarily H_2O_2 and to a lesser extent
168 superoxide and hydroxyl radicals (30) (Fig. 1A, B). ABA treatment also induced chloroplastic ROS
169 in wild type guard cells, albeit to a lower extent than the PAP treatment (Fig. 1B). To test whether
170 the effect of PAP on chloroplast ROS requires ABA, we investigated the PAP treatment in an *ost1-*
171 *2* background which is deficient in ABA signaling and does not show ABA-induced stomatal closure
172 (30, 31). PAP still induced chloroplast ROS in *ost1-2* (Fig. 1C) while ABA did not, suggesting that
173 PAP acts independently of ABA in the induction of chloroplast ROS.

174

175 Given PAP is reported to lower, not raise, chloroplast ROS in photosynthetic tissues we
176 investigated further the interaction between PAP and chloroplastic ROS using biochemical and
177 genetic tools. The chloroplast photosynthetic electron transport chain is a major source of ROS in
178 chloroplasts (1). Therefore, we attempted to attenuate the chloroplastic ROS burst using different
179 concentrations of the photosynthesis inhibitor 3-(3-4,-dichlorophenyl)-1,1-dimethylurea (DCMU) on
180 *Arabidopsis thaliana* (*Arabidopsis*) epidermal peels. As expected, we observed incremental
181 reduction of the effective PSII quantum yield (Y(II)) of mesophyll tissue in response to the
182 increasing concentrations of DCMU (Fig. S1); whereas Y(II) in the guard cells was below the
183 detection threshold. We used this decrease of Y(II) in the mesophyll to infer that Y(II) was similarly
184 decreased in the chloroplasts of guard cells given the similarity of chloroplast photosynthesis in
185 both cell types (32, 33). Inhibition of guard cell photosynthesis and chloroplastic ROS production at
186 10 μM DCMU decreased both ABA- and PAP-induced ROS accumulation in guard cells and guard
187 cell chloroplasts (Fig. 1B). This decreased ROS correlated with impaired ABA- or PAP-induced
188 stomatal closure when co-treated with a range of DCMU concentrations (Fig. 1D, S2). Intriguingly,
189 this PAP-induced ROS burst driven by the light reactions of photosynthesis was not associated
190 with any changes to the low light regime; that is, there was no requirement for co-treatment with
191 high light as would be typically expected for a chloroplast ROS burst.

192

193 To further test if chloroplastic PSI ROS contributes to PAP-mediated stomatal closure, we utilized
194 a thylakoid ascorbate peroxidase (tAPX) over-expressor (tAPX-OE) line (34). This transgenic line
195 has high levels of tAPX activity for catalyzing the reduction of chloroplastic H_2O_2 to water.
196 We hypothesized that increased scavenging of chloroplastic PSI ROS prevents PAP-mediated
197 stomatal closure. Indeed, PAP-mediated stomatal closure was inhibited in tAPX-OE in comparison
198 to wild type (Fig. 1E).

199

200 As chloroplast-nuclear proximity and H_2O_2 transfer between these compartments in photosynthetic
201 tissues have been proposed as a key signaling mechanism (5), we examined these processes in
202 the context of PAP signaling in specialized guard cells. Of the three to six chloroplasts per single
203 guard cell, one or two chloroplasts were typically associated with the junction between two guard
204 cells, two to three chloroplasts with the nucleus, and one or none in neither location (classed as
205 'other', Fig. S3). The number of chloroplasts associated at the junction, nucleus or 'other' location
206 was not affected by PAP treatment (Fig. S3). Significantly, PAP induced ROS to a similar extent in
207 all guard cell chloroplasts, including those associated with the nucleus (Fig. S4). We next examined
208 whether PAP also induces ROS accumulation in nuclei of guard cells. We found that PAP also
209 induced a ROS burst in the nucleus, to a higher degree than even the chloroplasts (Fig. 1C). Taken
210 together, our results indicate that PAP induces ROS production in guard cell chloroplasts, with the
211 ROS capable of accumulating to high levels in the nucleus and the theoretical possibility of it
212 occurring via chloroplast-to-nucleus H_2O_2 transfer.
213
214 *Apoplastic ROS production by RBOHD is required for PAP-mediated signaling processes*

215 While apoplastic ROS is required for stomatal closure mediated by ABA (35) the role and genetic
216 components for this process have not been identified for PAP-mediated stomatal closure. We found
217 that the double mutant *rbohDrbohF* (*rbohDF*) did not close in response to PAP and had the
218 expected impaired ABA-mediated stomatal closure (36) (Fig. 2A). Interestingly, we found
219 that single knockout *rbohF* mutant was responsive to PAP but had completely impaired ABA-
220 mediated stomatal closure (i.e., no different to the control). In contrast, ABA induced stomatal
221 closure in *rbohD*, but PAP could not. Indeed, while ABA induced a significant increase in ROS
222 of *rbohD* guard cells, PAP treatment on *rbohD* did not (Fig. 2B); this was also the case for when
223 chloroplastic ROS was specifically measured (Fig. 2B). This indicates that ABA induces ROS
224 via RBOHF whereas PAP acts through RBOHD, which marks an important delineation between
225 ABA- and PAP-mediated stomatal closure.
226

227 The requirement of RBOHD for PAP-induced chloroplastic ROS (Fig. 2B) would suggest that
228 production of plastidial ROS is initiated by extracellular ROS in this signaling cascade. We then
229 tested the reverse hypothesis, that is, apoplastic ROS production requires chloroplastic ROS.
230 Given the difficulty in distinguishing apoplastic ROS from cytosolic ROS of guard cells using
231 confocal microscopy images, we explored whether chloroplastic ROS contributed to other
232 apoplastic ROS processes influenced by PAP levels such as flg22-induced ROS. There was no
233 significant difference between wild type and the tAPX-OE line in response to flg22 (Fig. S5);
234 suggesting that chloroplastic ROS may not directly influence apoplastic ROS, at least for flg22-
235 associated ROS processes.
236
237 *PAP-induced CPKs activate RBOHD and SLAC1 thereby simultaneously impacting ROS and anion*
238 *currents in stomatal closure*
239 The induction of RBOHD activity for ROS production is thought to occur both by calcium transients
240 and protein kinase activation. Intracellular calcium binds to the EF-hand motifs of RBOH, while the
241 calcium influx can lead to the activation of several kinases such as the CPKs, which can
242 phosphorylate RBOHD at the N terminus (26). Considering PAP requires RBOHD to initiate
243 stomatal closure, we investigated potential CPK candidates shown to be transcriptionally up-
244 regulated by PAP (30) as enhancers of RBOHD-mediated ROS production.
245
246 To determine whether these candidate CPKs could enhance the ROS-producing activity of
247 RBOHD, we used the heterologous expression of human embryonic kidney 293T (HEK293T) cells,
248 which do not have endogenous NADPH oxidases (37). Measurement of ROS in these cells by
249 luminol-amplified chemiluminescence showed that the single transfections of CPKs alone did not
250 differ significantly to the non-transfection control, indicating that the CPKs alone could not
251 induce ROS production (Fig. S6). HEK293T cells were then co-transfected with *3FLAG-*
252 *RBOHD* and either *CPK-3Myc*, or *3Myc-GFP* as a negative control (Fig. 3A).
253 RBOHD protein levels were homogenous between co-transfections, indicating that any differences

254 in ROS production would be due to an additional protein partner (Fig. S6). Co-transfection
255 with CPK12, CPK28, CPK32 and CPK34 significantly enhanced RBOHD-mediated ROS
256 production in comparison to the control (Fig. 3A). CPK13 did not induce significantly different ROS
257 production compared to the control, despite CPK13 being expressed to higher levels than CPK28
258 or CPK32 in the HEK293T cells (Fig. S7). Overall, these results demonstrate that multiple, yet
259 specific, CPKs that are transcriptionally up-regulated by PAP can activate RBOHD for PAP-
260 mediated ROS functions.
261
262 Interestingly, the RBOHD-activating kinases include CPK32 and CPK34, which we have previously
263 identified as CPKs capable of activating SLAC1 in *Xenopus laevis* oocytes (30). This raises the
264 question of which, amongst the repertoire of PAP-upregulated CPKs, might target RBOHD and
265 SLAC1 together or individually. We therefore tested CPK8, CPK12, CPK13 and CPK28 for SLAC1
266 activation using the *Xenopus* heterologous expression system (Fig. 3B, S8-10). CPK12 could not
267 activate SLAC1 in oocytes, consistent with findings by Brandt et al. (38), nor could CPK28 elicit
268 SLAC1 anion currents. However, both CPK8 and CPK13 could elicit SLAC1 anion currents, albeit
269 to varying degrees in four independent experiments. Overall, different members of the PAP-induced
270 CPKs target RBOHD and SLAC1 either individually or collectively (Table S1).
271
272 Different kinases phosphorylate different serine sites on SLAC1 (13, 38, 39). Serine 120 (S120) is
273 phosphorylated by OST1, while CPK6 phosphorylates S59 (39). To define whether some of our
274 identified CPK candidates target these phosphorylation sites, S59 and S120 of SLAC1 were
275 individually or both mutated to alanine. SLAC1 S59A and SLAC1 S120A were individually co-
276 expressed in oocytes with CPK13, CPK32 and CPK34 (Fig. 3C, S10). Contrary to published
277 literature on OST1 and CPKs phosphorylating distinct sites on SLAC1, either one of the S59A or
278 S120A mutations in SLAC1 on its own led to a reduction in anion currents for CPK32 and CPK34.
279 When we mutated both serine sites (i.e., SLAC1-S59A:S120A), this led to a further reduction in
280 anion currents for CPK13 (Fig. S10). We validated these findings *in planta* by testing whether

281 different *Arabidopsis* SLAC1 mutants responded to PAP. As expected, PAP and ABA did not close
282 stomata of *slac1-4* lacking the SLAC1 protein (Fig. S11). Importantly, the *slac1-S59A/S120A*
283 double mutant which expresses SLAC1 containing mutated serine sites, did not close stomata
284 when treated with PAP (Fig. 3D).
285
286 Considering these PAP-related CPKs could activate both RBOHD and the anion channel SLAC1
287 individually, or both, thereby simultaneously impacting ROS and anion currents in stomatal closure,
288 we wanted to determine whether they could compensate for the lack of OST1, an important kinase
289 that activates SLAC1 and potentially RBOHF (11, 12). We expressed the different CPKs in the *ost1*
290 background and performed a water-loss assay on excised individual leaves of these transgenic
291 lines. We included CPK23, which is a known activator of SLAC1 (40) involved in the ABA signaling
292 pathway but not transcriptionally PAP-induced; expressing CPK23 in *ost1* did not alter the water-
293 loss rate when compared to the empty-vector *ost1* control (Fig. 3E). In contrast, the overexpression
294 of PAP-induced CPKs in *ost1* could reduce the water loss in comparison to empty-vector *ost1* to
295 varying degrees (Fig. 3E). This indicates that PAP-induced CPKs, and in particular for CPK32 and
296 CPK34, can at least partially replace the function of OST1 *in vivo* by modulating RBOHD and/or
297 SLAC1 activity (Table S1).
298
299 *PAP intersects with ROS signaling across diverse cell types and processes*
300 ROS, in particular H_2O_2, are critical secondary messengers in many cell types and cellular
301 processes. Therefore, we explored the extent to which PAP might intersect with ROS beyond the
302 guard cell. First, we investigated whether the characteristic ROS production induced by the
303 pathogen elicitor flg22 (20–22) is altered in *sal1* leaves as a whole, given that both flg22 and now
304 PAP (Fig. 2A) have been shown to act via RBOHD in guard cells. Flg22 induced a much more
305 pronounced 'initial' ROS burst in *sal1* in comparison to wild type (Fig. 4A), while the negative control
306 *rbohD* did not produce any ROS.
307

308 Ozone enters leaves via stomata, and is readily converted to secondary ROS including H_2O_2, super
309 oxide and hydroxyl radical in the apoplast (41). The whole-leaf response to ozone requires
310 functional OST1 (42) and perturbation of this response can result in excessive damage to vascular
311 tissue (43). Considering our previous finding that constitutive PAP signaling via *sal1* restores
312 stomatal closure in *ost1* (30), we investigated whether *ost1 sal1*-6 has restored ozone tolerance.
313 The ozone-tolerant wild type (ecotype Col-0) and ozone-sensitive *ost1* plants showed the expected
314 phenotypes, with lesions formed in the midrib of all leaves of *ost1* (Fig. S12). Interestingly, fewer
315 lesions developed on *ost1 sal1*-6; the lesions were primarily contained to the older leaves in the
316 lower part of the rosette. In accordance with this, whole plant electrolyte measurements showed
317 that the significantly greater extent of ozone-induced ion leakage in *ost1* was decreased to wild
318 type levels in *ost1 sal1-6* (Fig. 4B), indicating that PAP accumulation restores ozone tolerance, and
319 thereby ROS responses, in whole leaves lacking OST1.
320
321 We finally examined the effect of constitutive PAP accumulation on another cellular process which
322 utilize ROS production and/or signaling; namely cell-to-cell permeability via plasmodesmata, as
323 their aperture can be dynamically regulated by ROS in roots treated with exogenous H_2O_2 (44).
324 The *sal1* mutant alleles *sal1*-6 and *sal1*-8 showed more open plasmodesmata in comparison to
325 wild type, as indicated by greater diffusion of green fluorescent protein (GFP) from the initial particle
326 bombardment site into neighboring cells (Fig. 4C). Interestingly we identified several genes related
327 to plasmodesmata aperture regulation that were also differentially expressed in *sal1*-8 compared
328 to wild type (Table S2). Collectively, these results suggest the potential for PAP to intersect with
329 ROS signaling and homeostasis in diverse cellular processes.
330
331 **Discussion**

332 Unanswered questions in the fields of ROS and retrograde signaling revolve around functional
333 redundancy versus specificity of signals, as well as a second less commonly considered quandary
334 which is the spatio-temporal intersection and neofunctionalization of the different signals in

335 specialized cells. For instance, if chloroplastic H_2O_2 itself is exported to the nucleus for signaling
336 roles (5), why do plant cells require other H_2O_2-triggered retrograde signals? Furthermore, signaling
337 roles for chloroplastic and apoplastic ROS have conventionally been considered separately; thus,
338 whether and how they intersect has remained unclear. A more fundamental question is if retrograde
339 signaling is an important cellular mechanism from an evolutionary perspective, how does it intersect
340 with other stress signaling pathways? Does this differ in specialized cells, such as guard cells
341 versus established roles in mesophyll cells or vasculature bundles (one of the proposed sites for
342 sensory plastids), as is the case for hormones and secondary messages?
343
344 The induction of chloroplast PSI ROS in guard cells by PAP (Fig. 1) was initially surprising, since
345 PAP contributes to a reduction in ROS in vascular bundles. This is consistent with PAP being a
346 chloroplast ROS-triggered signal in foliar tissue (4) that leads to the quenching of excess ROS via
347 up-regulation of the H_2O_2 scavenger *APX2* in this tissue type (29). However, given that ABA also
348 induced guard cell chloroplastic ROS (Fig. 1, (45)), our observations could reflect cell type-specific
349 functionalization of chloroplasts. Interestingly, guard cells obtain energy and carbohydrates via
350 different routes from mesophyll chloroplasts for stomatal opening regulation, even though
351 chloroplasts from both cell types are photosynthetically competent (32, 33, 46). Guard cells also
352 have a higher proportion of chloroplasts associated with the nucleus (Fig. S3) compared to
353 mesophyll cells, where direct H_2O_2 transfer from chloroplasts to the nucleus was reported (5).
354 Perturbing increases in chloroplastic PSI ROS whether by DCMU or tAPX over-expression, also
355 prevents stomatal closure (Fig. 1B, D, E, S2). Taken together, it seems that chloroplastic PSI ROS
356 and photosynthesis *per se* play important roles in guard cell signaling, with PAP, ABA and
357 apoplastic ROS among the triggers for a burst in photosynthetic-generated ROS. More generally,
358 the chloroplast is necessary for the continual propagation of ROS signals across the leaf in
359 wounding responses (47); and the enhanced flg22 ROS burst in *sal1-6* (Fig. 4C) suggests
360 chloroplast signaling via PAP could be involved in leaf-level ROS propagation. Overall, our findings

361 are consistent with, and contribute to, the model of the sensory plastid, which proposes specialized
362 environmental-sensing roles for chloroplasts that differ by cell type (48).
363
364 How could chloroplast-sourced ROS affect stomatal closure? We would assume a synergistic
365 interaction with RBOH ROS facilitating the calcium release, thereby promoting activation of ion
366 channels via CPKs (49, 50). Of note, we also observed a concurrent increase in nuclear ROS in
367 response to PAP (Fig. 1C), which is consistent with an emerging understanding of a role for
368 transcription in stomatal function (30, 51). While well beyond the scope of this study one can
369 speculate that chloroplast-sourced ROS oxidizing guard cell nuclear proteins may alter protein
370 interactions, trafficking, conformation and function (52, 53). Mining of recent proteomics studies
371 identifying proteins with H_2O_2-sensitive cysteine residues (53, 54) revealed several nuclear proteins
372 involved in stomatal regulation (55, 56). This list includes CO_2 INSENSITIVE 1 (CIS1) which is
373 required for elevated intracellular bicarbonate-induced activation of S-type anion channel currents
374 for CO_2-induced stomatal closure (57). The diversity of these proteins opens new research avenues
375 for understanding chloroplastic ROS signaling.
376
377 Apart from direct ROS/retrograde signaling targets, an outstanding question remains; how does
378 chloroplastic ROS intersect with apoplastic ROS? We found that PAP cannot induce ROS
379 accumulation in the chloroplasts of *rbohD* (Fig. 2B), indicating that apoplastic ROS is required for
380 chloroplastic ROS accumulation, at least for stomatal closure. This is consistent with other findings,
381 where chloroplasts are a site of ROS accumulation in guard cells in response to ozone which
382 mimics apoplastic ROS (47). The inhibition of PAP-induced stomatal closure by DCMU (Fig. 1D)
383 identifies PSI as the likely origin of the chloroplastic ROS required for stomatal closure. It is unclear
384 how apoplastic ROS leads to perturbation of the photosynthetic electron transport chain, but one
385 possible pathway is via Ca^{2+}. We previously observed Ca^{2+} influx in guard cells treated with PAP
386 (58). Activation of the HPCA kinase by apoplastic ROS leads to influx of Ca^{2+} (18) which can
387 influence the activity of several PSI proteins and photoprotection mechanisms such as cyclic

388 electron flow, limiting photosynthetic ROS accumulation (59, 60) Identifying and understanding the
389 (likely complex) interactions and processes required for the activation and requirement for
390 chloroplastic ROS will be a significant future challenge.
391
392 Interestingly, some of the PAP-induced CPKs have multiple functions in the guard cell i.e.,
393 activating both RBOHD and SLAC1 (Table S1). While CPK13 could not activate RBOHD, it has
394 been shown to inhibit KAT1 and KAT2 inward potassium channels (61). Notably, the PAP-induced
395 CPKs activate SLAC1 through at least two phosphorylation sites, S59 and S120 (Fig. 3C, S10)
396 unlike the previously reported specificity of other CPKs for S59 and OST1 for S120 (39). The
397 multiplicity in target proteins and phosphosites of PAP-induced CPKs may translate to an additive
398 effect for stomatal regulation, since the CPKs identified to have multiple targets (i.e., CPK13,
399 CPK32 and CPK34) provided the greatest degree of complementation in preventing leaf water loss
400 when expressed in the *ost1* mutant background (Fig. 3E). The upregulation of these different CPKs
401 that are distinct to those involved in ABA signaling identifies PAP as a node that connects the
402 chloroplast, ROS and calcium signaling with ion channel activity for stomatal regulation.
403
404 Our finding that the induction of stomatal closure by PAP occurs via RBOHD but not RBOHF, while
405 ABA acts via RBOHF (Fig. 2) or RBOHD in some instances (64) provides a distinct delineation
406 between these two drought-induced signaling molecules and their downstream pathways.
407 However, this finding again raises the question of functional redundancy versus specificity of
408 cellular signals: why do guard cells utilize a chloroplast signaling pathway to close stomata, when
409 ABA is very effective at doing so? We previously showed that PAP accumulation compensates for
410 deficiency in ABA signaling; for example PAP closes stomata in otherwise ABA-insensitive mutants
411 such as *ost1* and *abi1*, as well as enhancing the effect of ABA-mediated seed germination
412 repression (30). Intriguingly, plants under prolonged water stress have reduced stomatal sensitivity
413 to ABA, which is exacerbated the longer the water stress (i.e. 24 hours vs 14 days) (62). During
414 drought in *Arabidopsis*, ABA accumulates rapidly (~1-3 days) compared to the slower buildup of

415 PAP (~7-9 days) (29). This temporal separation of ABA and PAP accumulation may be relevant. It
416 could lead to ABA activating particular CPKs and OST1 to produce ROS, Ca^{2+} and activate SLAC1
417 to close stomata in the earlier stages of drought. With prolonged drought stress, subsequent PAP
418 accumulation activates the parallel CPK-RBOHD-SLAC1 pathways described herein to maintain
419 stomatal closure. Taken together, this suggests that chloroplasts, via signals such as PAP, co-
420 regulate the same proteins targeted by ABA to provide a time-gated reinforcement mechanism for
421 stomatal regulation.
422
423 Analogous mechanisms for the intersection of chloroplast, ROS and Ca^{2+} signaling most likely exist
424 in multiple leaf cell types and across different cellular processes, since we observed enhanced
425 ROS production in response to flg22 in *sal1* with constitutively accumulated PAP (Fig. 4A). While
426 these observations may be explained by PAP-upregulated CPKs capable of accentuating the
427 RBOHD-mediated ROS burst, such a mechanism is unlikely to explain the effect of PAP
428 accumulation on increased plasmodesmal permeability (Fig. 4C), nor the aforementioned
429 decreased ROS in vascular bundles (29).
430
431 Our results herein contribute towards resolving enigmas pertaining to cell specialization. PAP
432 induces accumulation of both chloroplastic and apoplastic ROS; with both subcellular sources of
433 ROS being necessary for stomatal closure (Fig. 1–2). We establish the epistatic hierarchy of
434 signaling across the cell, with PAP-induced transcriptional up-regulation of CPKs enabling
435 activation of RBOHD for the apoplastic ROS burst, which in turn is required for the chloroplastic
436 ROS burst and stomatal closure (Fig. 3). The PAP-induced CPKs can target both RBOHD and the
437 anion channel SLAC1, including a SLAC1 phosphosite previously considered to be OST1-specific,
438 thus enabling bypass of the ABA-OST1 pathway for stomatal closure (Fig. 3). Finally, the effect of
439 PAP extends beyond guard cells as it intersects with ROS in diverse cell types and processes (Fig.
440 4). In conclusion we illustrate how chloroplast retrograde signals can intersect with and influence
441 multiple signaling pathways to regulate plant processes in a cell type-dependent manner.

442

443 **Materials and Methods**

444

445 Extended Methods and Materials are available in *SI Appendix*.

446

447 *Plant material*

448 *Arabidopsis thaliana* wild type used in this study is Columbia-0 (Col-0). Mutants and transgenic
449 lines are in the Col-0 background except for *ost1*-2, which is in the Landsberg erecta background.
450 Lines used in this study are *sal1*-6 (SALK_020882(29)); *sal1*-8 (CS66977; (29)); tAPX OE (34);
451 *ost1*-2 (*ost1*-2,(31)); *rbohD* (CS9555, (20)); *rbohF* (CS9557, (20)); *rbohDF* (CS9558, (20)); *slac1*-4
452 (SALK_137265, (43)); *slac1*-S59A/S120A (SLAC1 S59A/S120A; (39)), *ost1* (SALK_008068, (63)).
453 Candidate CPKs were transformed in the Col-0 *ost1* mutant using the agrobacterium transformation
454 floral dip method (64) and hygromycin screen (65), for candidates cloned in the pMDC32 binary
455 vector (66) with the cauliflower mosaic virus 35S promoter replaced with the guard cell promoter
456 pGC1 (67). For stomatal aperture, flg22 ROS and water-loss assays, *Arabidopsis* plants were
457 grown on soil with 16 h light at 22 °C, except for the *rboh* mutants and the respective Col-0 control,
458 which were grown at 12 h light. For confocal microscopy and ozone treatment assays, *Arabidopsis*
459 plants were grown on soil in 12 h light. For bombardment assays, *Arabidopsis* plants were grown
460 on soil with 10 h light at 22 °C.

461

462 *Microprojectile bombardment assays*

463 Bombardment assays of cytosolic GFP endoplasmic reticulum RFP (red fluorescent protein) were
464 performed as described in (68). Bombardment sites were imaged 16 hours after bombardment
465 using a confocal microscope (LSM Zeiss 800) with a 20× water dipping objective (W N-Achroplan
466 20×/0.5). GFP was excited with a 488 nm argon laser and collected at 505-530 nm, while RFP was
467 excited with a 561 nm DPSS laser and collected at 600-640 nm.

468

469 *Flg22-induced chemiluminescence ROS assay*

470 Chemiluminescence ROS assays were performed as described in (69). See extended methods.

471

472 *Ozone treatment*

473 Three-week-old *Arabidopsis* plants were exposed to 50 ppb ozone for six hours from 9:00 to 15:00.
474 Plants were then transferred back into the growth chamber, with damage visually being scored and
475 photographed 24 hours post exposure. For electrolyte leakage measurements, whole rosettes were
476 collected after the end of the ozone exposure (both ozone treated and those in the control condition,
477 i.e., plants left in the growth chamber at <20 ppb ozone) and placed into 20 mL of MilliQ H_2O.
478 Samples were measured using a Mettler conductivity meter (Model FE30) to obtain ion readings
479 24 hours post the initial ozone exposure. Samples were frozen completely, defrosted, and then
480 measurements were taken again to obtain total ion content, with values plotted as a % total ion
481 lost.

482

483 *Stomatal aperture assay*

484 Stomatal aperture assays were performed as per (30). See extended methods.

485

486 *Confocal microscopy*

487 Quantification of ROS in guard cells of epidermal peels was measured using 20 μM 2',7'-
488 dichlorodifluorescein diacetate (H_2DCFDA; Invitrogen) according to (30), with epidermal peels
489 treated as per (30). Fluorescence images were taken using a Leica inverted confocal microscope
490 using a 496-nm excitation line of an argon multiline laser. H_2DCFDA fluorescence emission was
491 detected at 505-525 nm, while chloroplast auto-fluorescence was detected at 680-700 nm. Images
492 were quantified using Fiji (NIH), with relative change in fluorescence of ROS determined with
493 images before and after treatment.

494

495 *HEK293T RBOHD ROS assay*

496 A prepared 96-well plate with HEK293T cells transfected with genes of interest (see extended
497 methods for cloning specifics, transfection protocol, and protein extraction and western blot
498 associated, adapted from (70)) was gently washed with 100 µL Hank's Balanced Salt Solution
499 [HBSS, with Ca^{2+} and Mg^{+}; ThermoFisher Scientific], and then 100 µL of the assay buffer [29.9 mL
500 HBSS, with Ca^{2+} and Mg^{+}, 90 µL of 0.002 g horseradish peroxidase dissolved in 100 µL HBSS
501 solution, 18.8 µL of 0.4 M luminol] was added to each well. The plate was put into a plate reader
502 capable of polarization mode dispersion to measure luminescence at 37 °C. First, luminescence
503 was measured for 15 minutes for cells only in the assay buffer [measurement time 1 s/well, interval
504 1 min/well], then 50 µL of 3 µM ionomycin solution dissolved in the assay buffer was dispensed in
505 each well and measured for another 15 minutes.
506
507 *Electrophysiology*
508 SLAC1-mediated anion currents in oocytes were performed as per (30). See extended methods.
509
510 *Statistical analyses*
511 Data presented as boxplots have the middle line marking the median, the box indicating the upper
512 and lower quartiles, and the whiskers showing the minimum and maximum values within 1.5×
513 interquartile range. Data were analyzed using RStudio 2021.09.01 Build 351/R version 4.0.3. See
514 extended methods for specifics.
515
516 **Acknowledgments**
517 We thank Professor Julian Schroeder for kindly providing the seeds of *slac1-S59A/S120A*. We
518 thank the Western Sydney University Confocal Bio-Imaging Facility for usage of the confocal
519 microscope. We thank Professor Wah Soon Chow (ANU) for guidance on usage of the DCMU
520 inhibitor. We received financial support from the ARC Laureate Fellowship (FL190100056 to BJP);
521 ANU scholarships (EET); ARC Discovery Early Career Researcher Award (DE210100466 to KXC);
522 ARC Future Fellowship (FT210100366 to ZHC); European Research Council (grant agreement

523 725459, “INTERCELLAR”) and the Biotechnology and Biological Research Council (Institute
524 Strategic Programme ‘Plant Health’ BBS/E/J/000PR9796) (AB and CF), Australian Endeavour
525 Award (6975_2018) and CSIRO Synthetic Biology Future Science Platform (MC), and the Academy
526 of Finland (decisions #275632, #28313, #312498 and #323917 for MW).

527

528 **References**

529 1. C. Waszczak, M. Carmody, J. Kangasjärvi, Reactive Oxygen Species in Plant Signaling.
530 *https://doi.org/10.1146/annurev-arplant-042817-040322* **69**, 209–236 (2018).

531 2. S. R. Cutler, P. L. Rodriguez, R. R. Finkelstein, S. R. Abrams, Abscisic Acid: Emergence of a
532 Core Signaling Network. *https://doi.org/10.1146/annurev-arplant-042809-112122* **61**,
533 651–679 (2010).

534 3. K. X. Chan, S. Y. Phua, P. Crisp, R. McQuinn, B. J. Pogson, Learning the Languages of the
535 Chloroplast: Retrograde Signaling and Beyond. *Annu Rev Plant Biol* **67**, 25–53 (2016).

536 4. K. X. Chan, *et al.*, Sensing and signaling of oxidative stress in chloroplasts by inactivation
537 of the SAL1 phosphoadenosine phosphatase. *Proc Natl Acad Sci U S A* **113**, E4567–E4576
538 (2016).

539 5. M. Exposito-Rodriguez, P. P. Laissue, G. Yvon-Durocher, N. Smirnoff, P. M. Mullineaux,
540 Photosynthesis-dependent H2O2 transfer from chloroplasts to nuclei provides a high-
541 light signalling mechanism. *Nature Communications 2017 8:1* **8**, 1–11 (2017).

542 6. T. Maruta, *et al.*, H2O2-triggered Retrograde Signaling from Chloroplasts to Nucleus Plays
543 Specific Role in Response to Stress. *J Biol Chem* **287**, 11717 (2012).

544 7. S. Y. Park, *et al.*, Abscisic acid inhibits type 2C protein phosphatases via the PYR/PYL
545 family of START proteins. *Science* **324**, 1068–1071 (2009).

546 8. Y. Ma, *et al.*, Regulators of PP2C phosphatase activity function as abscisic acid sensors.
547 *Science* **324**, 1064–1068 (2009).

548 9. C. Belin, *et al.*, Identification of Features Regulating OST1 Kinase Activity and OST1
549 Function in Guard Cells. *Plant Physiol* **141**, 1316–1327 (2006).

550 10. R. Yoshida, *et al.*, The regulatory domain of SRK2E/OST1/SnRK2.6 interacts with ABI1 and
551 integrates abscisic acid (ABA) and osmotic stress signals controlling stomatal closure in
552 Arabidopsis. *J Biol Chem* **281**, 5310–5318 (2006).

553 11. C. Sirichandra, *et al.*, Phosphorylation of the Arabidopsis AtrbohF NADPH oxidase by
554 OST1 protein kinase. *FEBS Lett* **583**, 2982–2986 (2009).

555 12. B. R. Acharya, B. W. Jeon, W. Zhang, S. M. Assmann, Open Stomata 1 (OST1) is limiting in
556 abscisic acid responses of Arabidopsis guard cells. *New Phytol* **200**, 1049–1063 (2013).

557 13. D. Geiger, *et al.*, Activity of guard cell anion channel SLAC1 is controlled by drought-stress
558 signaling kinase-phosphatase pair. *Proc Natl Acad Sci U S A* **106**, 21425–21430 (2009).

559 14. D. Imes, *et al.*, Open stomata 1 (OST1) kinase controls R-type anion channel QUAC1 in
560 Arabidopsis guard cells. *Plant J* **74**, 372–382 (2013).

561 15. A. Sato, *et al.*, Threonine at position 306 of the KAT1 potassium channel is essential for
562 channel activity and is a target site for ABA-activated SnRK2/OST1/SnRK2.6 protein
563 kinase. *Biochem J* **424**, 439–448 (2009).

564 16. Z. M. Pei, *et al.*, Calcium channels activated by hydrogen peroxide mediate abscisic acid
565 signalling in guard cells. *Nature 2000 406:6797* **406**, 731–734 (2000).

566 17. Y. Wang, Z. H. Chen, B. Zhang, A. Hills, M. R. Blatt, PYR/PYL/RCAR Abscisic Acid Receptors
567 Regulate K+ and Cl− Channels through Reactive Oxygen Species-Mediated Activation of
568 Ca2+ Channels at the Plasma Membrane of Intact Arabidopsis Guard Cells. *Plant Physiol*
569 **163**, 566–577 (2013).

570 18. F. Wu, *et al.*, Hydrogen peroxide sensor HPCA1 is an LRR receptor kinase in Arabidopsis.
571 *Nature 2020 578:7796* **578**, 577–581 (2020).

572 19. M. M. Drerup, *et al.*, The Calcineurin B-like calcium sensors CBL1 and CBL9 together with
573 their interacting protein kinase CIPK26 regulate the Arabidopsis NADPH oxidase RBOHF.
574 *Mol Plant* **6**, 559–569 (2013).

575 20. M. A. Torres, J. L. Dangl, J. D. G. Jones, Arabidopsis gp91phox homologues Atrbohd and
576 Atrbohf are required for accumulation of reactive oxygen intermediates in the plant
577 defense response. *Proc Natl Acad Sci U S A* **99**, 517–522 (2002).

578 21. J. Morales, Y. Kadota, C. Zipfel, A. Molina, M. A. Torres, The Arabidopsis NADPH oxidases
579 RbohD and RbohF display differential expression patterns and contributions during plant
580 immunity. *J Exp Bot* **67**, 1663–1676 (2016).

581 22. L. Li, *et al.*, The FLS2-Associated Kinase BIK1 Directly Phosphorylates the NADPH Oxidase
582 RbohD to Control Plant Immunity. *Cell Host Microbe* **15**, 329–338 (2014).

583 23. M. Zhang, *et al.*, The MAP4 Kinase SIK1 Ensures Robust Extracellular ROS Burst and
584 Antibacterial Immunity in Plants. *Cell Host Microbe* **24**, 379-391.e5 (2018).

585 24. D. H. Lee, *et al.*, Regulation of reactive oxygen species during plant immunity through
586 phosphorylation and ubiquitination of RBOHD. *Nat Commun* **11** (2020).

587 25. X. Gao, *et al.*, Bifurcation of Arabidopsis NLR Immune Signaling via Ca2+-Dependent
588 Protein Kinases. *PLoS Pathog* **9**, e1003127 (2013).

589 26. U. Dubiella, *et al.*, Calcium-dependent protein kinase/NADPH oxidase activation circuit is
590 required for rapid defense signal propagation. *Proc Natl Acad Sci U S A* **110**, 8744–8749
591 (2013).

592 27. P. A. Crisp, *et al.*, RNA Polymerase II Read-Through Promotes Expression of Neighboring
593 Genes in SAL1-PAP-XRN Retrograde Signaling. *Plant Physiol* **178**, 1614–1630 (2018).

594 28. P. A. Crisp, *et al.*, Rapid Recovery Gene Downregulation during Excess-Light Stress and
595 Recovery in Arabidopsis. *Plant Cell* **29**, 1836–1863 (2017).

596 29. G. M. Estavillo, *et al.*, Evidence for a SAL1-PAP Chloroplast Retrograde Pathway That
597 Functions in Drought and High Light Signaling in Arabidopsis. *Plant Cell* **23**, 3992–4012
598 (2011).

599 30. W. Pornsiriwong, *et al.*, A chloroplast retrograde signal, 3'phosphoadenosine 5'-
600 phosphate, acts as a secondary messenger in abscisic acid signaling in stomatal closure
601 and germination. *Elife* **6** (2017).

602 31. A. C. Mustilli, S. Merlot, A. Vavasseur, F. Fenzi, J. Giraudat, Arabidopsis OST1 protein
603 kinase mediates the regulation of stomatal aperture by abscisic acid and acts upstream
604 of reactive oxygen species production. *Plant Cell* **14**, 3089–3099 (2002).

605 32. T. Lawson, K. Oxborough, J. I. L. Morison, N. R. Baker, The responses of guard and
606 mesophyll cell photosynthesis to CO2, O2, light, and water stress in a range of species are
607 similar. *J Exp Bot* **54**, 1743–1752 (2003).

608 33. T. Lawson, S. Lefebvre, N. R. Baker, J. I. L. Morison, C. A. Raines, Reductions in mesophyll
609 and guard cell photosynthesis impact on the control of stomatal responses to light and
610 CO2. *J Exp Bot* **59**, 3609 (2008).

611 34. I. Murgia, *et al.*, Arabidopsis thaliana plants overexpressing thylakoidal ascorbate
612 peroxidase show increased resistance to Paraquat-induced photooxidative stress and to
613 nitric oxide-induced cell death. *Plant J* **38**, 940–953 (2004).

614 35. O. Rodrigues, *et al.*, Aquaporins facilitate hydrogen peroxide entry into guard cells to
615 mediate ABA- and pathogen-triggered stomatal closure. *Proc Natl Acad Sci U S A* **114**,
616 9200–9205 (2017).

617 36. J. M. Kwak, *et al.*, NADPH oxidase AtrbohD and AtrbohF genes function in ROS-
618 dependent ABA signaling in Arabidopsis. *EMBO J* **22**, 2623–2633 (2003).

619 37. B. Bánfi, *et al.*, A Ca2+-activated NADPH Oxidase in Testis, Spleen, and Lymph Nodes.
620 *Journal of Biological Chemistry* **276**, 37594–37601 (2001).

621 38. B. Brandt, *et al.*, Reconstitution of abscisic acid activation of SLAC1 anion channel by
622 CPK6 and OST1 kinases and branched ABI1 PP2C phosphatase action. *Proc Natl Acad Sci*
623 *U S A* **109**, 10593–10598 (2012).

624 39. B. Brandt, *et al.*, Calcium specificity signaling mechanisms in abscisic acid signal
625 transduction in Arabidopsis guard cells. *Elife* **4**, e03599 (2015).

626 40. D. Geiger, *et al.*, Guard cell anion channel SLAC1 is regulated by CDPK protein kinases
627 with distinct Ca2+ affinities. *Proceedings of the National Academy of Sciences* **107**, 8023
628 LP – 8028 (2010).

629 41. J. P. Vainonen, J. Kangasjärvi, Plant signalling in acute ozone exposure. *Plant Cell Environ*
630 **38**, 240–252 (2015).

631 42. T. Vahisalu, *et al.*, Ozone-triggered rapid stomatal response involves the production of
632 reactive oxygen species, and is controlled by SLAC1 and OST1. *The Plant Journal* **62**, 442–
633 453 (2010).

634 43. T. Vahisalu, *et al.*, SLAC1 is required for plant guard cell S-type anion channel function in
635 stomatal signalling. *Nature* **452**, 487 (2008).

636 44. H. L. Rutschow, T. I. Baskin, E. M. Kramer, Regulation of Solute Flux through
637 Plasmodesmata in the Root Meristem. *Plant Physiol* **155**, 1817–1826 (2011).

638 45. S. Iwai, *et al.*, Guard cell photosynthesis is crucial in abscisic acid-induced stomatal
639 closure. *Plant Direct* **3**, 1–10 (2019).

640 46. S. L. Lim, *et al.*, Arabidopsis guard cell chloroplasts import cytosolic ATP for starch
641 turnover and stomatal opening. *Nature Communications 2022 13:1* **13**, 1–13 (2022).

642 47. J. H. Joo, S. Wang, J. G. Chen, A. M. Jones, N. V. Fedoroff, Different signaling and cell
643 death roles of heterotrimeric G protein alpha and beta subunits in the Arabidopsis
644 oxidative stress response to ozone. *Plant Cell* **17**, 957–970 (2005).

645 48. S. A. Mackenzie, P. M. Mullineaux, Plant environmental sensing relies on specialized
646 plastids. *J Exp Bot* **73**, 7155–7164 (2022).

647 49. V. Demidchik, S. Shabala, Mechanisms of cytosolic calcium elevation in plants: the role of
648 ion channels, calcium extrusion systems and NADPH oxidase-mediated "ROS-Ca2+ Hub."
649 *Funct Plant Biol* **45**, 9–27 (2018).

650 50. M. Sierla, C. Waszczak, T. Vahisalu, J. Kangasjärvi, Reactive Oxygen Species in the
651 Regulation of Stomatal Movements. *Plant Physiol* **171**, 1569–1580 (2016).

652 51. F. Simeoni, *et al.*, The AtMYB60 transcription factor regulates stomatal opening by
653 modulating oxylipin synthesis in guard cells. *Scientific Reports 2022 12:1* **12**, 1–12 (2022).

654 52. J. Couturier, K. Chibani, J. P. Jacquot, N. Rouhier, Cysteine-based redox regulation and
655 signaling in plants. *Front Plant Sci* **4**, 105 (2013).

656 53. B. Wei, *et al.*, Identification of Sulfenylated Cysteines in Arabidopsis thaliana Proteins
657 Using a Disulfide-Linked Peptide Reporter. *Front Plant Sci* **11**, 777 (2020).

658 54. J. Huang, *et al.*, Mining for protein S-sulfenylation in Arabidopsis uncovers redox-
659 sensitive sites. *Proc Natl Acad Sci U S A* **116**, 20256–20261 (2019).

660 55. K. Tõldsepp, *et al.*, Mitogen-activated protein kinases MPK4 and MPK12 are key
661 components mediating CO2-induced stomatal movements. *The Plant Journal* **96**, 1018–
662 1035 (2018).

663 56. Q. Chen, *et al.*, COP1 promotes ABA-induced stomatal closure by modulating the
664 abundance of ABI/HAB and AHG3 phosphatases. *New Phytologist* **229**, 2035–2049
665 (2021).

666 57. J. He, *et al.*, The BIG protein distinguishes the process of CO2-induced stomatal closure
667 from the inhibition of stomatal opening by CO2. *New Phytologist* **218**, 232–241 (2018).

668 58. C. Zhao, *et al.*, Evolution of chloroplast retrograde signaling facilitates green plant
669 adaptation to land. *Proc Natl Acad Sci U S A* **116** (2019).

670 59. A. K. Hochmal, S. Schulze, K. Trompelt, M. Hippler, Calcium-dependent regulation of
671 photosynthesis. *Biochimica et Biophysica Acta (BBA) - Bioenergetics* **1847**, 993–1003
672 (2015).

673 60. Q. Wang, S. Yang, S. Wan, X. Li, The Significance of Calcium in Photosynthesis. *Int J Mol*
674 *Sci* **20** (2019).

675 61. E. Ronzier, *et al.*, CPK13, a noncanonical Ca2+-dependent protein kinase, specifically
676 inhibits KAT2 and KAT1 shaker K+ channels and reduces stomatal opening. *Plant Physiol*
677 **166**, 314–326 (2014).

678 62. Z. Y. Peng, J. D. B. Weyers, Stomatal sensitivity to abscisic acid following water deficit
679 stress. *J Exp Bot* **45**, 835–845 (1994).

680 63. R. Yoshida, *et al.*, ABA-Activated SnRK2 Protein Kinase is Required for Dehydration Stress
681 Signaling in Arabidopsis. *Plant Cell Physiol* **43**, 1473–1483 (2002).

682 64. S. J. Clough, A. F. Bent, Floral dip: a simplified method for Agrobacterium-mediated
683 transformation of Arabidopsis thaliana. *Plant J* **16**, 735–743 (1998).

684 65. S. J. Harrison, *et al.*, A rapid and robust method of identifying transformed Arabidopsis
685 thaliana seedlings following floral dip transformation. *Plant Methods* **2**, 1–7 (2006).

686 66. M. D. Curtis, U. Grossniklaus, A Gateway Cloning Vector Set for High-Throughput
687 Functional Analysis of Genes in Planta. *Plant Physiol* **133**, 462 (2003).

688 67. Y. Yang, A. Costa, N. Leonhardt, R. S. Siegel, J. I. Schroeder, Isolation of a strong
689 Arabidopsis guard cell promoter and its potential as a research tool. *Plant Methods* **4**, 1–
690 15 (2008).

691 68. E. E. Tee, S. Samwald, C. Faulkner, Quantification of Cell-to-Cell Connectivity Using
692 Particle Bombardment. 263–272 (2022).

693 69. M. Albert, M. Butenko, R. Aalen, G. Felix, M. Wildhagen, Chemiluminescence Detection
694 of the Oxidative Burst in Plant Leaf Pieces. *Bio Protoc* **5** (2015).

695 70. S. Kimura, H. Kaya, K. Hashimoto, M. Wrzaczek, K. Kuchitsu, Quantitative Analysis
696 for ROS-Producing Activity and Regulation of Plant NADPH Oxidases in HEK293T
697 Cells. *Methods in Molecular Biology* **2526**, 107–122 (2022).

698 **Figures and Tables**

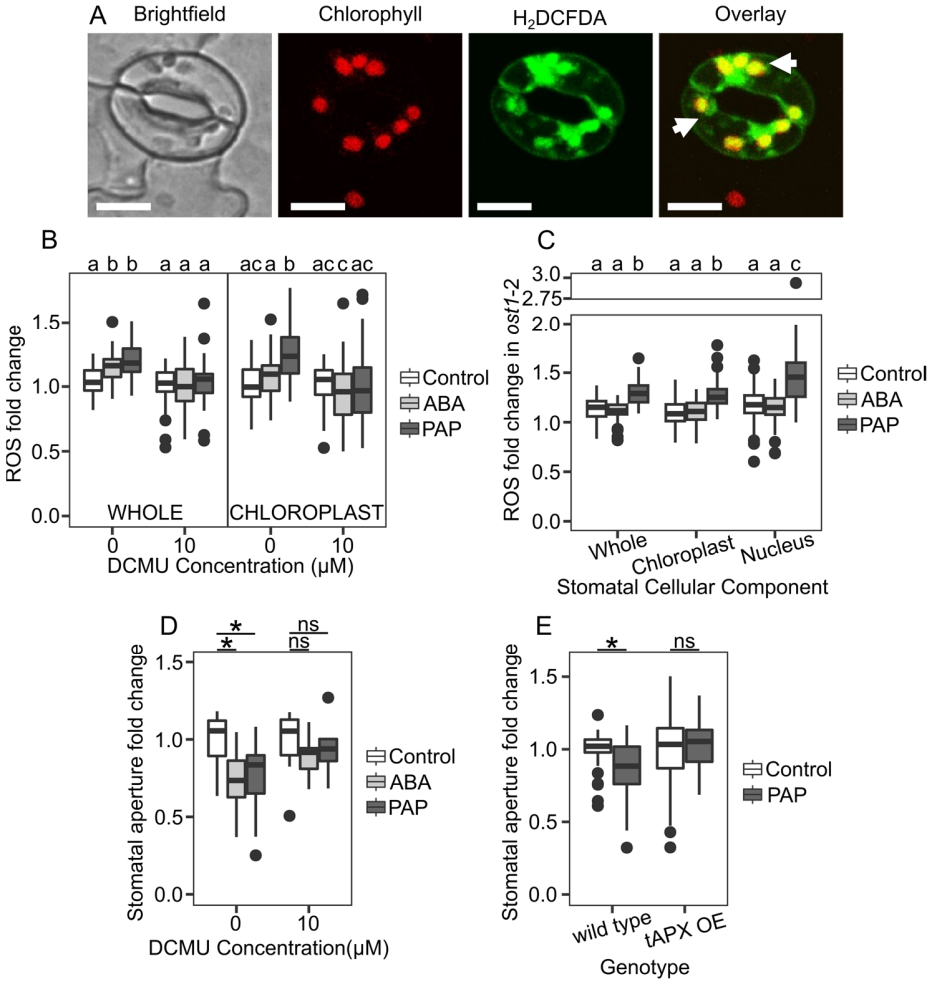

699

700 **Figure 1. Subcellular compartmentalization of ROS intersects with retrograde PAP signaling**

701 (A) Localization of ROS within guard cells with arrows indicating ROS at chloroplasts. Scale bars

702 = 10 μM. (B) and (E) show relative change in fluorescence (compared to control) in different parts

703 of the stomata after treatment (100 μM ABA or 100 μM PAP). Fluorescence is an indication of ROS

704 levels as per the ROS dye H_2DCFDA. (B) shows the relative change in fluorescence in whole guard

705 cells or guard cell chloroplasts after treatments with or without 10 μM DCMU. Each condition

706 contains a minimum of three wild type plants with n ≥ 49 stomata per treatment combination. For

707 'Whole', factors 'DCMU' and 'Treatment' significantly impacted fluorescence with a significant

708 interaction between the two (ANOVA; F =59.6, df=1, p<0.001; F=12.0, df=2, p<0.001; F = 7.3, df=2,

709 $p<0.001$). Significant differences from the respective control denoted by a and b. For 'Chloroplast',
710 factors 'DCMU' and 'Treatment' significantly impacted fluorescence, with a significant interaction
711 between the two (ANOVA; $F = 32.7$, $df=1$, $p<0.001$; $F=23.7$, $df=2$, $p<0.001$; $F=11.6$, $df=2$, $p<0.001$).
712 Significant differences from the respective control denoted by a, b or c. For (C), each
713 treatment/subcellular component combination contains a three *ost1*-2 plants with a minimum of n
714 ≥ 40 stomata. 'Treatment' and 'Part' significantly impacted fluorescence (ANOVA; $F=68.8$, $df=2$,
715 $p<0.001$ and $F=13.4$, $df=2$ $p<0.001$), with a significant interaction between the two (ANOVA; $F=3.2$,
716 $df=4$, $p<0.05$). Significant differences denoted by a, b and c. (D) Stomatal aperture in response to
717 100 µM ABA or 100 µM PAP with 0 or 10 µM DCMU, fold change relative to DCMU control (i.e., 0
718 DCMU or 10 µM DCMU). Each condition contains a minimum of three wild type plants with a
719 minimum of n ≥ 27 stomata per treatment combination. 'DCMU' and 'Treatment' significantly
720 impacted closure (ANOVA; $F=7.7$, $df=1$, $p<0.01$; $F=4.2$, $df=2$, $p<0.05$), with significant differences
721 from respective control determined denoted by *, $p < 0.05$. (E) Stomatal closure in response to 100
722 µM PAP in tAPX OE. Each condition contains a minimum of three biological replicates with a
723 minimum of n ≥ 41 stomata per treatment combination. 'Genotype' significantly impacted closure
724 (ANOVA; $F= 5.4$, $df=1$, $p<0.05$), with a significant interaction between 'Genotype' and 'Treatment'
725 (ANOVA; $F=4.9$, $df=1$, $p<0.05$). Significant differences from the genotype control denoted by *,
726 $p<0.05$.
727

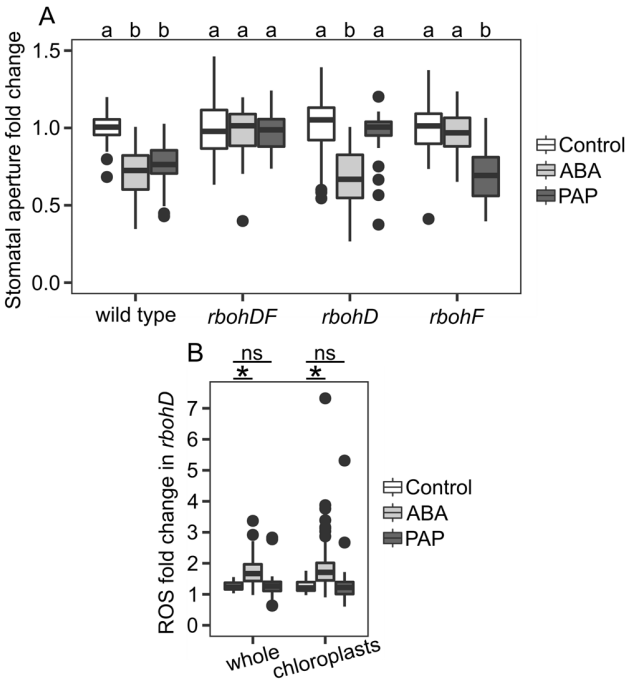

728

729 **Figure 2. *rboh* mutants are differentially perturbed in ABA and PAP-mediated stomatal**
730 **closure**

731 (A) Stomatal closure of *rboh* mutants in response to 100 μM ABA or 100 μM PAP. Each condition
732 contains a minimum of three biological replicates with a minimum of n ≥ 34 stomata per treatment
733 combination. 'Genotype' and 'Treatment' significantly impacted closure with an interaction between
734 the two (ANOVA; F=15.8, df=3, p<0.001; F=38.6, df=2, p<0.001; F=18.1, df=6, p<0.001).
735 Significant differences to the respective genotype control denoted by a or b. (B) Relative change in
736 fluorescence in whole or chloroplasts of *rbohD* guard cells as an indication of ROS levels. Each
737 condition contains a minimum of three biological replicates with a minimum of n ≥ 38 stomata per
738 treatment combination. 'Treatment' significantly impacted fluorescence in both 'whole' and
739 'chloroplasts' datasets (ANOVA; F=16.5, df=2, p<0.01; F=7.4, df=2, p<0.05), with significant
740 differences from the controls denoted by *, p<0.05.

741

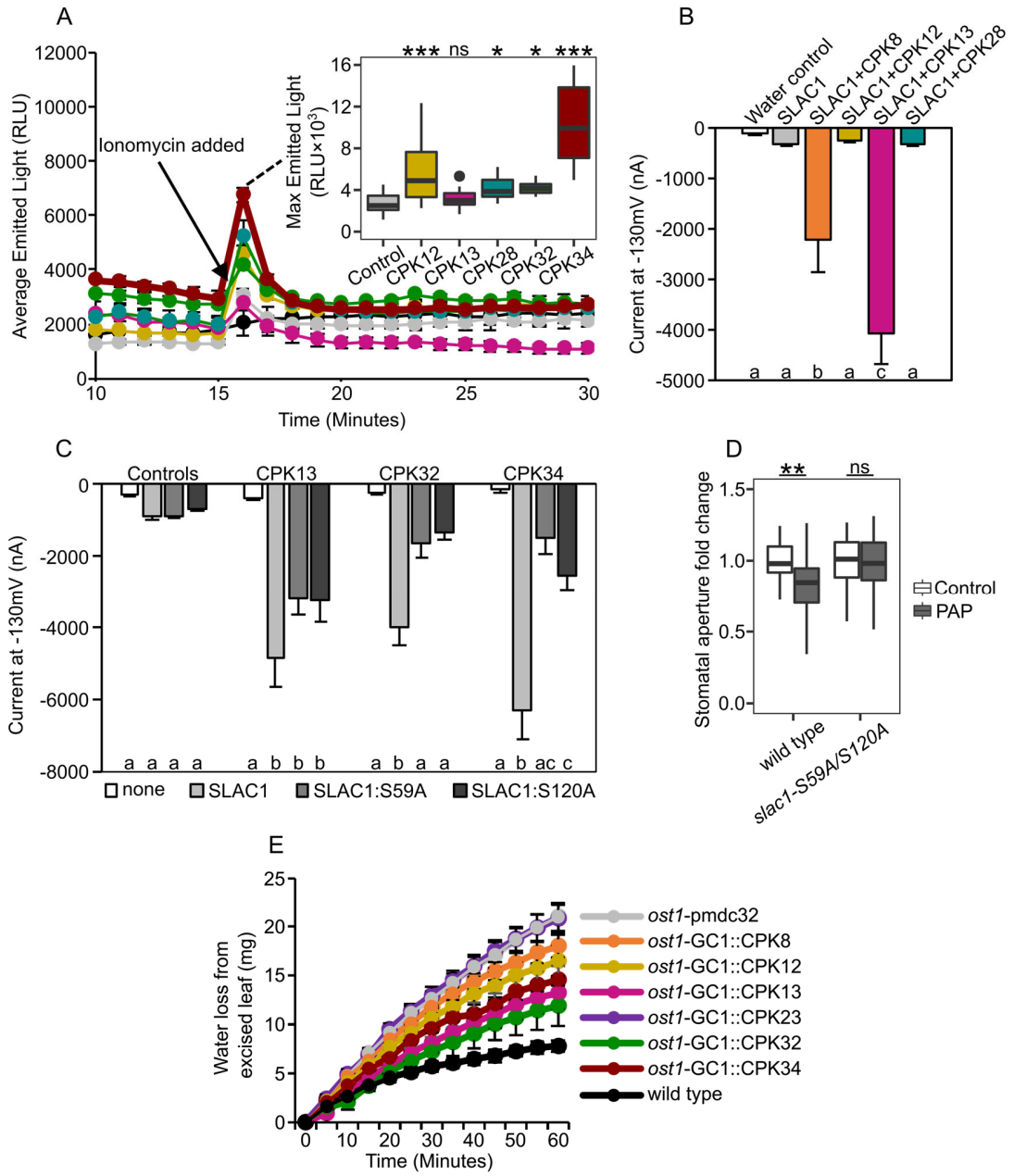

742

743 **Figure 3. Different PAP-induced CPKs enhance RBOHD-mediated ROS production and**

744 **SLAC1 anion currents**

745 (A) ROS production of HEK293T cells transiently expressing CPKs with RBOHD. After 15 min 1

746 μM ionomycin was added to the medium. Values represent mean ± SEM for either three non-

747 transfected replicates (shown in black), RBOHD co-transfected with GFP (control) or designated
748 CPK. The experiment was repeated in at least four independent experiments with similar results;
749 boxplot shows average max emitted light with data pooled from separate experiments. Control n =
750 24, CPK12 n = 18, CPK13, 28, 32, and 34 n = 12. Factor 'Gene' expressed with RBOHD
751 significantly impacted the max emitted light after ionomycin was added (ANOVA; F=32.3, df=5,
752 p<0.001), with significant differences from the control denoted as * for p<0.05 or *** for p<0.0001.
753 (B) CPK8, CPK12, CPK13 and CPK28 activation of SLAC1 anion channel in oocytes. Values are
754 means of four to eight oocytes ± SEM. Anion channel activity shown as steady state currents
755 activated at -130 mV, with significant differences between injected combinations (ANOVA; F=3.5,
756 df=5, p<0.01), denoted by a, b and c. Experiment was repeated on positive candidates in two other
757 batches of oocytes. See Fig. S7 for full trace. (C) Anion currents of mutated phosphosites in SLAC1
758 when co-expressed with CPK13, CPK32 and CPK34 in oocytes. Values are from a minimum of five
759 oocytes per combination ± SEM. Factors 'Type of SLAC1 expressed' and 'CPK' expressed
760 significantly impacted the anion currents, with a significant interaction between the two (ANOVA;
761 F=70.8, df=3, p<0.001; F=33.5, df=3, p<0.001; F=16.8, df=9, p<0.001). Significant differences with
762 a given CPK expressed denoted by a, b and c. (D) Stomatal aperture of *slac1-S59A/S120A* mutant
763 in response to 100 μM PAP. Each has a minimum of three biological replicates with a minimum of
764 n ≥ 31 stomata per genotype/treatment combination. Factors 'Genotype' and 'Treatment'
765 significantly impacted closure with a significant interaction between the two (ANOVA; F=6.3, df=1,
766 p<0.05; F=6.4, df=1, p<0.05; F = 5.5, df=1, p<0.05). Significant differences from the genotype
767 control denoted by **, p<0.01. (E) Water loss assay in excised leaves of *ost1* complemented with
768 guard-cell promoter expressed CPKs. Independent transgenics lines, where n = 8, 17, 14, 9, 13, 6,
769 14 and 11 respectively for *ost1*-pmdc32, *ost1*-GC::CPK8, *ost1*-GC::CPK12, *ost1*-GC::CPK13, *ost1*-
770 GC::CPK23, *ost1*-GC::CPK32, *ost1*-GC::CPK34, and wild type.

771

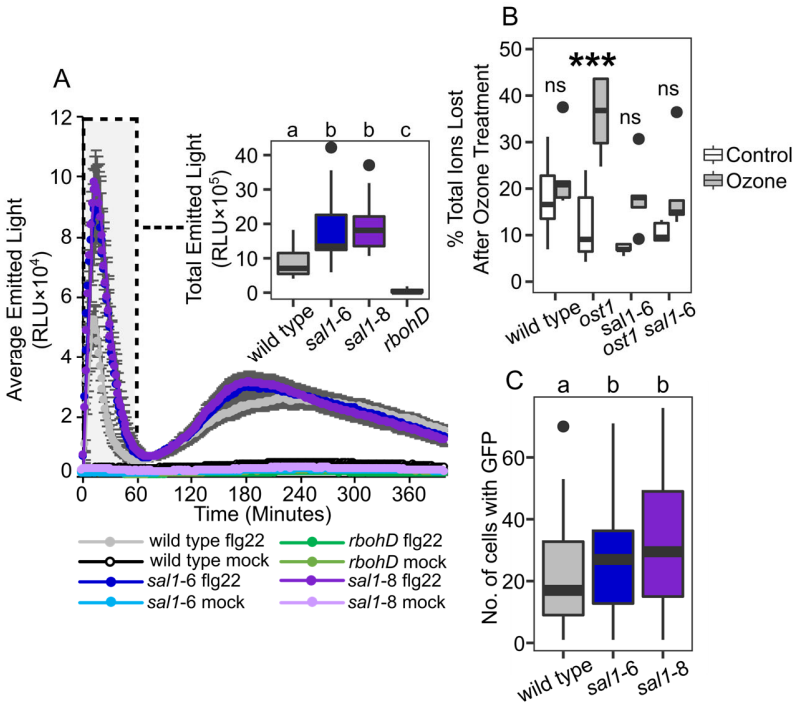

Figure 4. Altered cellular ROS processes in *sal1 mutant.*

(A) Flg22 chemiluminescence response kinetics in Arabidopsis *sal1* mutant leaf discs. Average of five-week-old plants ± SEM (eight per genotype and treatment), with data combined from two separate experiments (n=16). Boxplot shows total emitted light over 60 minutes for wild type, *sal1*-6 and *sal1*-8 and *rbohD* in response to flg22. Independent factor 'Genotype' was determined as significant (ANOVA; F=36.6, df=3, p<0.001); significant differences between genotypes denoted by a, b and c. (B) Electrolyte leakage measurements from plants harvested after six-hour exposure to ozone, 24 hours after start of ozone exposure. Values are plotted as a % total ion lost, with n = 5 per genotype and treatment. Factors 'Genotype' and 'Treatment' had a significant impact on total ion lost (ANOVA; F=4.7, df=3, p<0.01 and F=25.5, df=1, p<0.001), with significant differences between treatments within a genotype denoted by ***, p<0.001. (C) Microprojectile bombardment into leaf tissue of *sal1*-6, *sal1*-8 and wild type show *sal1* mutants have more GFP movement to neighboring cells than wild type. Number of bombardment sites counted ≥84 per genotype, three leaves × three different plants per genotype. Experiment repeated with similar significant trends found. Significance differences between genotypes indicated by a and b.